

# Image Inpainting: Theoretical Analysis and Comparison of Algorithms

Emily J. King<sup>a</sup>, Gitta Kutyniok<sup>a</sup>, and Wang-Q Lim<sup>a</sup>

<sup>a</sup> Institute of Mathematics, Technische Universität Berlin, Berlin, Germany

## ABSTRACT

An issue in data analysis is that of incomplete data, for example a photograph with scratches or seismic data collected with fewer than necessary sensors. There exists a unified approach to solving this problem and that of data separation: namely, minimizing the norm of the analysis (rather than synthesis) coefficients with respect to particular frame(s). There have been a number of successful applications of this method recently. Analyzing this method using the concept of clustered sparsity leads to theoretical bounds and results, which will be presented. Furthermore, necessary conditions for the frames to lead to sufficiently good solutions will be shown, and this theoretical framework will be used to show that shearlets are able to inpaint larger gaps than wavelets. Finally, the results of numerical experiments comparing this approach to inpainting to numerous others will be presented.

**Keywords:** inpainting,  $\ell_1$  minimization, shearlets, sparse representations, data recovery, frames

## 1. INTRODUCTION

Repairing holes in objects is an important problem in both the analog and the digital realm. Conservators, who mend scratches and other damage to paintings, call the process inpainting. This term is now also applied to the process of filling in missing gaps in digital images and even audio. A certain sparsity-driven approach to inpainting, which will be outlined in this paper, bridges the gap between the analog (continuous) and digital (discrete) domains. It has been theoretically shown in [KKZ13, KKZ11] that this approach, using shearlets in a particular way to inpaint a particular continuous-domain model inspired by a common problem in seismology, outperforms using wavelets. In what follows, a number of different inpainting methods will be applied to a selection of different types of holes in different types of images in the discrete domain. Analysis-side shearlet inpainting in general outperforms the other methods in these examples. The general theoretical inpainting method of [KKZ13, KKZ11] will be presented in Section 2. Both wavelets and shearlets are then used with this method to inpaint a particular model inspired by seismic data. Shearlets are shown to outperform. Other inpainting approaches such as non-local means are discussed in Section 3. Finally, Section 4 contains the results of numerical experiments comparing various approaches.

## 2. INPAINTING VIA ANALYSIS-SIDE $\ell_1$ -MINIMIZATION

### 2.1 Notation

We first introduce the notation used in the paper. A collection of vectors  $\Phi = \{\varphi_i\}_{i \in I}$  in a separable Hilbert space  $\mathcal{H}$  forms a *Parseval frame* for  $\mathcal{H}$  if for all  $x \in \mathcal{H}$ ,

$$\sum_{i \in I} |\langle x, \varphi_i \rangle|^2 = \|x\|^2.$$

---

Send correspondence to Emily J. King, gnikylime@gmail.com.

Further contact information: Gitta Kutyniok, kutyniok@math.tu-berlin.de, +49 (0)30 314-25758 ; Wang-Q Lim, lim@math.tu-berlin.de, +49 (0)30 314 ? 25751

With a slight abuse of notation, given a Parseval frame  $\Phi$ , we also use  $\Phi$  to denote the *synthesis operator*

$$\Phi : \ell_2(I) \rightarrow \mathcal{H}, \quad \Phi(\{c_i\}_{i \in I}) = \sum_{i \in I} c_i \varphi_i.$$

With this notation,  $\Phi^*$  is called the *analysis operator*.

Given a space  $X$  and a subset  $A \subseteq X$ , we will use the notation  $A^c$  to denote  $X \setminus A$ . Also, the *indicator function*  $\mathbb{1}_A$  is defined to take the value 1 on  $A$  and 0 on  $A^c$ .

## 2.2 Problem formulation

Given a Hilbert space  $\mathcal{H} = \mathcal{H}_K \oplus \mathcal{H}_M$ , the (noiseless) inpainting problem can in general be posed as wanting to find  $x^0 \in \mathcal{H}$  given knowledge of  $P_K x^0$ , where  $P_K$  is the orthogonal projection onto  $\mathcal{H}_K$ .

$$(\text{INP}_0) \quad x^* \in \mathcal{H} \text{ subject to } P_K x^* = P_K x^0.$$

This is clearly an underdetermined problem. Some other constraint must be introduced in order to solve the problem. For example, very natural class of images to consider is that of cartoon-like images.

**Definition 1.** We define the space of *cartoon-like images*  $\mathcal{C}$  to be

$$\mathcal{C} = \{f \in L^2([0, 1]^2) : f = f_1 + f_2 \mathbb{1}_\Omega, f_1, f_2 \in C^2, \partial\Omega \text{ piecewise } C^2\}.$$

That is,  $\mathcal{C}$  consists loosely of smooth patches separated by piecewise smooth boundaries. So one might reasonably assume that  $x^0$  is cartoon-like. Then the inpainting problem can be reposed as finding  $x^0 \in \mathcal{C}$  given  $P_K x^0$ .

$$(\text{INP}_1) \quad x^* \in \mathcal{C} \text{ subject to } P_K x^* = P_K x^0.$$

However, this problem is not very tractable in its current form. Sparsity-based approaches to problem solving have been shown to be very successful in a number of different applications, particular in signal and image processing (see, for example, [SMF10]). In this case, it has been shown [KL12, GK13] that particular collections of vectors yield (almost) optimally sparse representations of cartoon-like images.

**Definition 2.** (GK13) A *parameterization* is a mapping of a discrete index set  $\Lambda$  to  $\mathbb{R}_+ \times \mathbb{T} \times \mathbb{R}^2$  defined as  $\lambda \mapsto (s_\lambda, \theta_\lambda, x_\lambda)$ . Assume  $\Lambda$  has a parameterization. Let

$$R_\theta = \begin{pmatrix} \cos(\theta) & -\sin(\theta) \\ \sin(\theta) & \cos(\theta) \end{pmatrix}$$

denote the rotation matrix of angle  $\theta$  and  $D_a = \text{diag}(a, \sqrt{a})$  the anisotropic dilation matrix with  $a > 0$ . A family  $(m_\lambda)_{\lambda \in \Lambda}$  is called a *family of parabolic molecules of order*  $(P, M, N_1, N_2)$  if it can be written as

$$m_\lambda(x) = 2^{3s_\lambda/4} a^{(\lambda)} (D_{2^{s_\lambda}} R_{\theta_\lambda} (x - x_\lambda))$$

such that

$$\left| \partial^\beta \hat{a}^{(\lambda)}(\xi) \right| \lesssim \min \left( 1, 2^{-s_\lambda} + |\xi_1| + 2^{-s_\lambda/2} |\xi_2| \right)^M \langle |\xi_1| \rangle^{-N_1} \langle \xi_2 \rangle^{-N_2}$$

for all  $|\beta| \leq P$ . The implicit constants are uniform over  $\lambda \in \Lambda$ .

With some light constraints on  $\Lambda$ ,  $P$ ,  $M$ ,  $N_1$ , and  $N_2$  and assuming that a family of parabolic molecules  $(m_\lambda)_{\lambda \in \Lambda}$  is a frame, then the frame has an almost optimal best  $N$ -term approximation rate for cartoon images [GK13]. The concept of parabolic molecules was introduced as a means of explaining a number of similar results that had been proving concerning two classes of systems, curvelets and shearlets. Here we will focus on Parseval frames of shearlets. The canonical shearlet systems are called *cone-adapted shearlets* [GKL06].

**Definition 3.** The *cone-adapted shearlet system*  $\mathcal{SH}(\phi, \psi, \tilde{\psi})$  generated by  $\phi \in L^2(\mathbb{R}^2)$  and  $\psi, \tilde{\psi} \in L^2(\mathbb{R}^2)$  is the union of  $\{\phi(\cdot - \ell) : \ell \in \mathbb{Z}^2\}$ ,  $\{2^{3j/4}\psi(S_k A_{2^j} \cdot - \ell) : j \geq 0, |k| \leq \lceil 2^{j/2} \rceil, \ell \in \mathbb{Z}^2\}$ , and  $\{2^{3j/4}\tilde{\psi}(\tilde{S}_k \tilde{A}_{2^j} \cdot - \ell) : j \geq 0, |k| \leq \lceil 2^{j/2} \rceil, \ell \in \mathbb{Z}^2\}$ , where

$$A_a = \begin{pmatrix} a & 0 \\ 0 & \sqrt{a} \end{pmatrix} \text{ and } S_\ell = \begin{pmatrix} 1 & \ell \\ 0 & 1 \end{pmatrix}.$$

The shearing and anisotropic dilations have the effect of moving the supports of the Fourier transform of the two generating shearlets in a way that decomposes the frequency domain in an almost polar manner, as illustrated in Figure 1. It is known that, modulo some smoothness conditions, cone-adapted shearlet systems

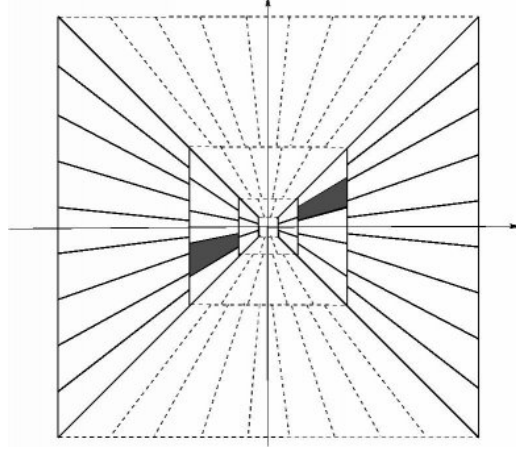


Figure 1. Shearlet tiling of the frequency plane

are parabolic molecules [GK13]. Given this new machinery, we could state the inpainting problem as

$$(\text{INP}_2) \quad x^* = \Phi c^*, c^* = \operatorname{argmin}_c \|c\|_1 \text{ subject to } P_K \Phi c = P_K x^0.$$

However, we will instead state it as

$$(\text{INP}) \quad x^* = \operatorname{argmin}_x \|\Phi^* x\|_1 \text{ subject to } P_K x = P_K x^0.$$

There are a number of reasons why we would consider  $(\text{INP}_2)$  [*synthesis-side inpainting*] instead of  $(\text{INP})$  [*analysis-side inpainting*]. An important feature of Parseval frames is that for all  $x \in \mathcal{H}$ ,  $\Phi \Phi^* x = x$ . However, for all Parseval frames which are not bases, there are infinitely many such  $c$  which satisfy  $\Phi c = x$ . So numerical instabilities could arise when attempting to solve  $(\text{INP}_2)$ . Furthermore, the *analysis sequence*  $\Phi^* x$  minimizes the  $\ell_2$  norm over all possible *synthesis coefficients*  $c$ . Namely,

$$\Phi^* x = \operatorname{argmin}_c \|c\|_2 \text{ subject to } c \in \ell_2, x = \Phi c.$$

Thus,  $(\text{INP})$  may also be regarded as a mixed  $\ell_1 - \ell_2$  problem [KT09]. One may view the optimization problem in  $(\text{INP})$  as a relaxation of the *cosparsity* problem

$$x^* = \operatorname{argmin}_x \|\Phi^* x\|_0 \text{ subject to } P_K x = P_K x^0.$$

Theoretical results concerning cosparsity may be found in [NDEG11, NDEG13]. Finally,  $(\text{INP})$  is similar to the algorithmic approaches to inpainting found in [KKZ11] and [Kut03].

Although we motivated the formulation of the statement of  $(\text{INP})$  using cartoon-like images and shearlets, it works well whenever the desired object  $x^0 \in \mathcal{H}$  belongs to a class which has a sparse representation with respect to a Parseval frame  $\Phi$ .

There is a similarly motivated formulation of the inpainting problem using one-step thresholding of the analysis coefficients in [KKZ11]. For the sake of brevity, we omit it here.

### 2.3 Theoretical guarantees

We now introduce two important notions,  $\delta$ -clustered sparsity and cluster coherence, which in some sense measure whether or not a particular Parseval frame  $\Phi$  is appropriate to use in (INP).

**Definition 4.** Fix  $\delta > 0$ . Given a Hilbert space  $\mathcal{H}$  with a Parseval frame  $\Phi = \{\varphi_i\}_{i \in I}$ ,  $x \in \mathcal{H}$  is  $\delta$ -clustered sparse in  $\Phi$  (with respect to  $\Lambda \subseteq I$ ) if

$$\|\mathbb{1}_{\Lambda^c} \Phi^* x\|_1 \leq \delta.$$

**Definition 5.** Let  $\Phi_1 = \{\varphi_{1i}\}_{i \in I}$  and  $\Phi_2 = \{\varphi_{2j}\}_{j \in J}$  lie in a Hilbert space  $\mathcal{H}$  and let  $\Lambda \subseteq I$ . Then the cluster coherence  $\mu_c(\Lambda, \Phi_1; \Phi_2)$  of  $\Phi_1$  and  $\Phi_2$  with respect to  $\Lambda$  is defined by

$$\mu_c(\Lambda, \Phi_1; \Phi_2) = \max_{j \in J} \sum_{i \in \Lambda} |\langle \varphi_{1i}, \varphi_{2j} \rangle|.$$

Cluster coherence was introduced in [DK13] to apply to the geometric separation problem and may be seen as a further development of mutual coherence [DH01] and earlier notions of coherence adapted to the clustering of frame vectors [DE03, Tro04, BGN08]. Cluster coherence and clustered sparsity were first used in conjunction with the inpainting problem in [KKZ11, KKZ13]. These notions may be used to show theoretical guarantees of successful inpainting.

**Proposition 6.** (KKZ13) Fix  $\delta > 0$  and suppose that  $x^0$  is  $\delta$ -clustered sparse in  $\Phi$ . Let  $x^*$  solve (INP). Then

$$\|x^* - x^0\|_2 \leq \frac{2\delta}{1 - 2\mu_c(\Lambda, P_M \Phi; \Phi)}.$$

Both clustered sparsity and cluster coherence depend on the chosen set of indices  $\Lambda$ . However,  $\Lambda$  is merely a tool to determine when  $\Phi$  is a good dictionary for inpainting and explicit knowledge of it is not necessary to recover missing data. In fact, one may reword Proposition 6 as

**Proposition 7.** Fix  $\delta > 0$  and suppose that  $x^0$  is  $\delta$ -clustered sparse in  $\Phi$  for at least one index set  $\Lambda$ . Let  $x^*$  solve (INP). Then

$$\|x^* - x^0\|_2 \leq \min_{\Lambda} \left\{ \frac{2\delta}{1 - 2\mu_c(\Lambda, P_M \Phi; \Phi)} : \mu_c(\Lambda, P_M \Phi; \Phi) < 1/2, \|\mathbb{1}_{\Lambda^c} \Phi^* x\|_1 \leq \delta \right\}.$$

A heuristic explanation of the proposition is as follows: If  $\Phi$  is a “good” dictionary to use, then there is a small set of analysis coefficients, enumerated by a  $\Lambda$ , which contain most of the information of  $x^0$  (i.e.,  $\|\mathbb{1}_{\Lambda^c} \Phi^* x\|_1 \leq \delta$ ) and those elements of  $\Phi$  which capture that information do not fall too much into the hole of missing data (i.e.,  $\mu_c(\Lambda, P_M \Phi; \Phi)$  is small). Again, there are similar theoretical guarantees for inpainting using one-step thresholding (see [KKZ11]).

### 2.4 A comparison of shearlets and wavelets

It was already mentioned above that shearlets (nearly) optimally sparsely represent cartoon-like images. It is known that wavelet representations of natural images are compressible [Cev09], but they do not approximate cartoon-like images as well as shearlets [KL12]. This would lead one to believe that Parseval frames of shearlets would inpaint more successfully than wavelets. In a particular model, this can be shown to be true. Certain one dimensional wavelets are associated with two different kinds of functions, a scaling function  $\Phi$  and a mother wavelet  $\psi$ . These functions are commonly used to create two dimensional wavelet systems.

**Definition 8.** A 2D wavelet system is defined to be

$$\{\Phi(\cdot - \ell) : \ell \in \mathbb{Z}^2\} \cup \{2^j \psi^\iota(2^j \cdot - \ell) : j \geq 0, \ell \in \mathbb{Z}^2, \iota \in \{v, h, d\}\},$$

where  $\Phi(x) = \phi(x_1)\phi(x_2)$ ,  $\psi^v(x) = \phi(x_1)\psi(x_2)$ ,  $\psi^h(x) = \psi(x_1)\phi(x_2)$ , and  $\psi^d(x) = \psi(x_1)\psi(x_2)$ .

Wavelet systems are formed using isotropic dilation and translations while shearlet systems are formed using anisotropic dilation, shearing, and translations. The anisotropy allows shearlets to better pick up curvilinear features.

We now present a quick summary of the model that shearlets provably asymptotically inpaint better than wavelets. For the ease of exposition, many of the details have been omitted. They may be found in [KKZ13]. Since cartoon-like images are governed by edges, the image to be inpainted is a masked linear singularity. The distribution  $w\mathcal{L}$  acting on Schwartz functions  $g \in \mathcal{S}'(\mathbb{R}^2)$  is defined by

$$\langle w\mathcal{L}, g \rangle = \int_{-\rho}^{\rho} w(x_1)g(x_1, 0)dx_1,$$

where  $w$  is a smooth weight and  $\rho > 0$ . Essentially, the weight  $w$  sets up the linear singularity that is smooth in the vertical direction, while the value of  $\rho$  corresponds to the length of the singularity. We mask the linear singularity (weighted distribution)  $w\mathcal{L}$  with the mask

$$M_h = \{(x_1, x_2) \in \mathbb{R}^2 : |x_1| \leq h\}, h > 0.$$

The observed signal is

$$f = \mathbb{1}_{\mathbb{R}^2 \setminus M_h} \cdot w\mathcal{L},$$

which is depicted in Figure 2 We decompose  $w\mathcal{L}$  by the same subbands  $F_j$ ,  $w\mathcal{L} \mapsto w\mathcal{L}_j = w\mathcal{L} * F_j$ , denote

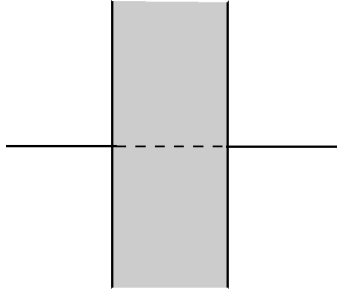


Figure 2.  $w\mathcal{L}$  masked by  $M_h$

$h = h_j$ , and set

$$f_j = \mathbb{1}_{\mathbb{R}^2 \setminus M_{h_j}} \cdot w\mathcal{L}_j.$$

Let  $\{\psi_\lambda\}_\lambda$  denote a particular wavelet Parseval frame (defined in [KKZ13]) and  $\{\sigma_\eta\}_\eta$  a particular shearlet Parseval frame. Then we can rewrite (Inp as

$$W_j = \operatorname{argmin}_{\tilde{W}_j} \|(\langle \tilde{W}_j, \psi_\lambda \rangle)_\lambda\|_1 \text{ s.t. } f_j = \mathbb{1}_{\mathbb{R}^2 \setminus M_{h_j}} \cdot \tilde{W}_j$$

for wavelet-based inpainting and

$$S_j = \operatorname{argmin}_{\tilde{S}_j} \|(\langle \tilde{S}_j, \sigma_\eta \rangle)_\eta\|_1 \text{ s.t. } f_j = \mathbb{1}_{\mathbb{R}^2 \setminus M_{h_j}} \cdot \tilde{S}_j$$

for shearlet-based inpainting. Now we can state the main result of [KKZ13].

**Theorem 9.** For  $h_j = o(2^{-j})$  (this is critical in thresholding case) as  $j \rightarrow \infty$ ,

$$\frac{\|W_j - w\mathcal{L}_j\|_2}{\|w\mathcal{L}_j\|_2} \rightarrow 0, \quad j \rightarrow \infty.$$

For  $h_j = o(2^{-j/2})$  as  $j \rightarrow \infty$ ,

$$\frac{\|S_j - w\mathcal{L}_j\|_2}{\|w\mathcal{L}_j\|_2} \rightarrow 0, \quad j \rightarrow \infty.$$

Thus, shearlets are able to asymptotically inpaint over wider masks than wavelets.

### 3. REVIEW OF OTHER INPAINTING METHODS

The main inpainting methods in the literature may be categorized as being sparsity-based, variational, and patch-based. Sparsity-based methods involve a combination of harmonic analysis with convex optimization which may be viewed as (Inp), (Inp<sub>2</sub>), or something inbetween, possibly using a union of Parseval frames as a sparsifying dictionary, which is regularized (see, for example, [CCS10, DJL<sup>+</sup>12, ESQD05]). For example, the minimization task in [ESQD05] is

$$x^* = x_1^* + x_2^*, \quad (x_1^*, x_2^*) = \operatorname{argmin}_{x_1, x_2} \|\Phi_1^* x_1\|_1 + \|\Phi_2^* x_2\|_1 + \lambda \|P_M(x^0 - x_1 - x_2)\|_2^2 + \gamma \operatorname{TV}\{x_2\},$$

where  $\Phi_1$  is a Parseval frame consisting of parabolic molecules,  $\Phi_2$  is an oscillatory Parseval frame like DCT, Gabor, or wavelet packets, and  $\lambda, \gamma > 0$  are parameters. The algorithm used is based on the block-coordinate-relaxation method. When numerically testing shearlet-based analysis-side inpainting against other methods in Section 4, we will actually employ something much simpler (but still get good results) – namely, we use basic iterative thresholding on the analysis coefficients generated using dual shearlet frames constructed by two of the authors [KL].

Image processing literature is filled with a multitude of variational methods. Any list of papers will be incredibly incomplete, so we only mention a few [BBC<sup>+</sup>01, BBS01, BSCB00, CS02]. The book [Wei98] also contains an overview of PDE-based image processing. The core idea of variational-based inpainting is that information is propagated from the boundary of the holes along isophotes (edges) in the image to fill them in. For example, a common variational approach is to numerically solve the PDE

$$\frac{\partial I}{\partial t} = \nabla^\perp I \cdot \nabla \Delta I,$$

where  $I$  is the image intensity inside the region to be inpainted,  $\nabla$  is the gradient,  $\nabla^\perp$  is the perpendicular gradient  $(-\partial_y, \partial_x)$ , and  $\Delta$  is the Laplace operator. Many of the methods are inspired by real physical processes, like diffusion, osmosis, and fluid dynamics. It is interesting to note that there is a way to interpret a particular type of total variational inpainting as a limit of a certain type of analysis-side inpainting [CDOS12].

In patch- or exemplar-based inpainting, information is also propagated from the edge(s) of the missing data inward. However, in contrast to the variational approaches, the hole is iteratively filled using patches or averages of patches from other parts of the image. Specifically, in non-local means inpainting, the value of a reconstructed target pixel is a linear combination of values from patches with the coefficients of the combination determined by a weighted similarity function. Some examples of exemplar-based inpainting are [CPT04, LMM11, WO08, BCM06].

### 4. NUMERICAL RESULTS

In this section, we present a number of examples comparing various inpainting methods. In most cases, analysis-side iterative thresholding with shearlets outperforms the other methods, even though it is a primitive algorithm. To promote fair comparisons, the various parameters were not “tweaked;” that is, the shearlet-based inpainting was implemented the same in each example. In Figure 3, blocks of size  $32 \times 32$  pixels were removed from a grayscale Barbara image. The blocks were inpainted using the methods from [KL] and also [ESQD05]. The signal to noise ratio (SNR) for the former is 27.82 dB and the latter is 27.82 dB. This is surprising because as parabolic molecules, shearlets and curvelets share a number of performance guarantees. However, the results concerning parabolic molecules hold true asymptotically with a constant, so it is feasible that in practice one dictionary could outperform the other.

Figure 4 shows pictorially what one would expect given Theorem 9. Namely, when using iterative thresholding to inpaint an image which consists almost completely of curvilinear features, shearlets outperform wavelets. This figure first appeared in [KKZ13].

In Figure 5,  $32 \times 32$  blocks are masked out as in Figure 3, but the starting image is RGB rather than grayscale. Four inpainting methods are compared. Exemplar-based inpainting (article [CPT04], implementation [Bha]), non-local means inpainting (article [BCM06], implementation [NLM]), TV inpainting (article



Figure 3. (Upper Left) Original image (Upper Right)  $32 \times 32$  missing blocks (Lower Left) Curvelets+Local cosine (26.22 dB) [ESQD05] (Lower Right) Shearlets (27.82 dB)

[GO], implementation [Get]), and shearlet-based iterative thresholding. The first three methods were applied directly to the color image, while the shearlet-based inpainting was performed channel by channel. Even though the shearlet method involves inpainting the image three times (one for each channel), the corresponding run time was faster than the other methods. Further, the SNR is the best. Visually, the image inpainted with shearlets also looks the best, with the main problem area being the chin, but none of the inpainting methods successfully inpainted the chin.

$32 \times 32$  blocks are also masked out in Figure 6, but these blocks, while they have approximately the same density as the masked-out blocks in Figure 5, occur at random positions. The same inpainting methods as above (exemplar-based, non-local means, TV, and shearlet) are compared. This is the only example in the paper for which using the shearlet-based inpainting method does not outperform the other methods. The reason that the shearlet-inpainted image appears so washed out is that values much larger than 255 occurred in the “inpainted” version (the greenish spots). In order to display the image, it had to be normalized, which caused the non-problematic pixels to appear faint. What is additionally interesting is that the green spots appear in parts of the image that were not masked out. However, the run time is still shorter than the TV and non-local means approaches, so perhaps changing the exit criteria of the code will improve the performance.

Figure 7 contains seismic data taken from [Sei] which has been masked vertically, replicating missing acquisition sensors. Apparent memory leaks in both the implementation of exemplar inpainting and TV inpainting prevented a comparison of these methods on this image. Note that although the shearlet-based inpainting has a better SNR than the non-local means inpainting, it took about 3 times longer to run.

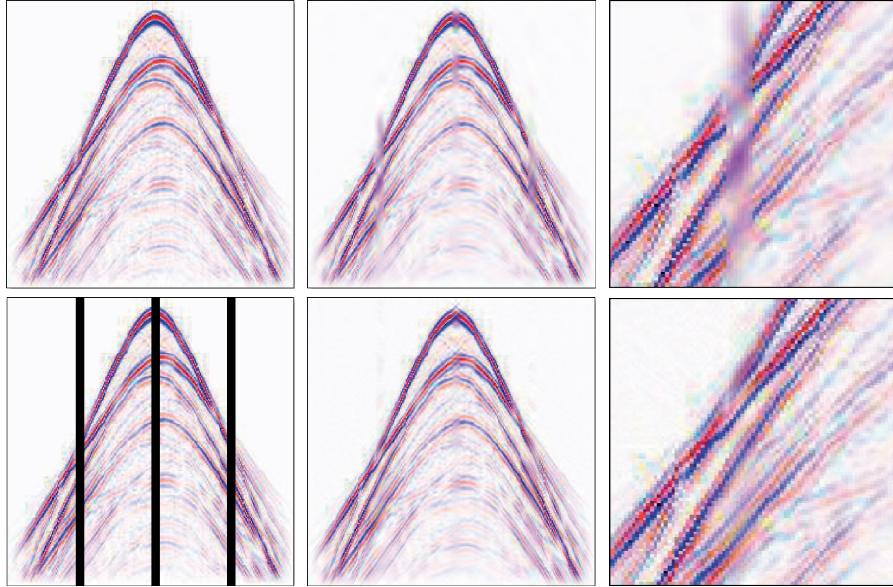


Figure 4. Top row, from left to right: original image, masked image inpainted with wavelets using iterative thresholding, detail of the wavelet inpainting. Bottom row, from left to right: image with the masked-out parts marked in black, masked image inpainted with shearlets using iterative thresholding, detail of the shearlet inpainting

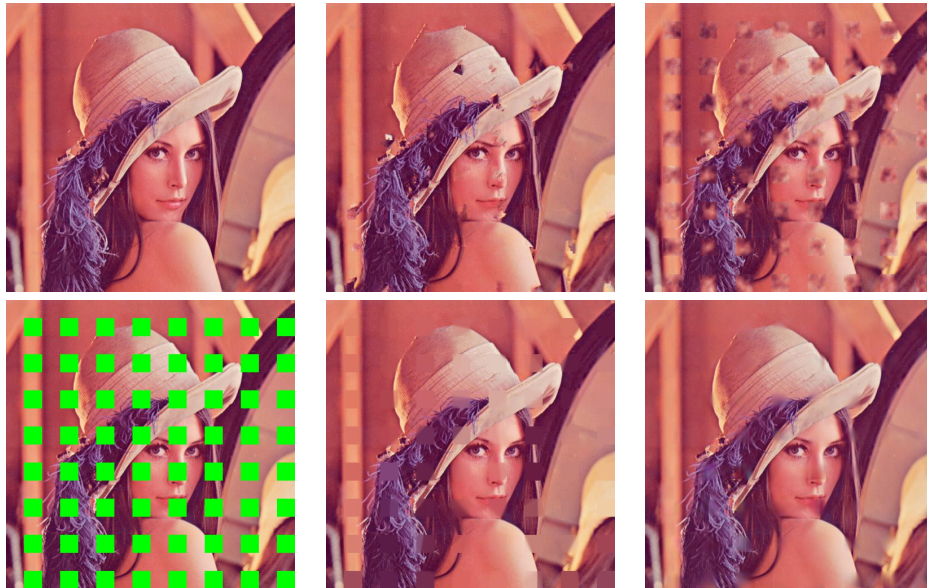


Figure 5. Top row, from left to right:  $512 \times 512$  RGB Lena, exemplar-based inpainting [CPT04, Bha] ( $t = 1723$  s, SNR = 20.306 dB), non-local means inpainting [BCM06, NLM] ( $t = 2038$  s, SNR = 17.568 dB). Bottom row from left to right:  $32 \times 32$  masked out, TV approach [GO, Get] ( $t = 6869$  s, SNR = 21.046 dB), shearlet-based iterative thresholding ( $t = 911$  s, SNR = 23.643 dB)

These results, coupled with the theoretical work, indicate that shearlet-based inpainting could be a very powerful approach. The next step will be to streamline the code and make it available on Shearlab.org



Figure 6. Top row, from left to right:  $512 \times 512$  RGB Lena, exemplar-based inpainting [CPT04, Bha] ( $t = 783.79$ s, SNR = 19.803 dB), non-local means inpainting [BCM06, NLM] ( $t = 6696.7$  s, SNR = 16.750dB). Bottom row from left to right: random  $32 \times 32$  masked out, TV approach [GO, Get] ( $t = 10200$  s, SNR = 19.995 dB), shearlet-based iterative thresholding ( $t = 2015.1$  s, SNR = 17.468 dB)

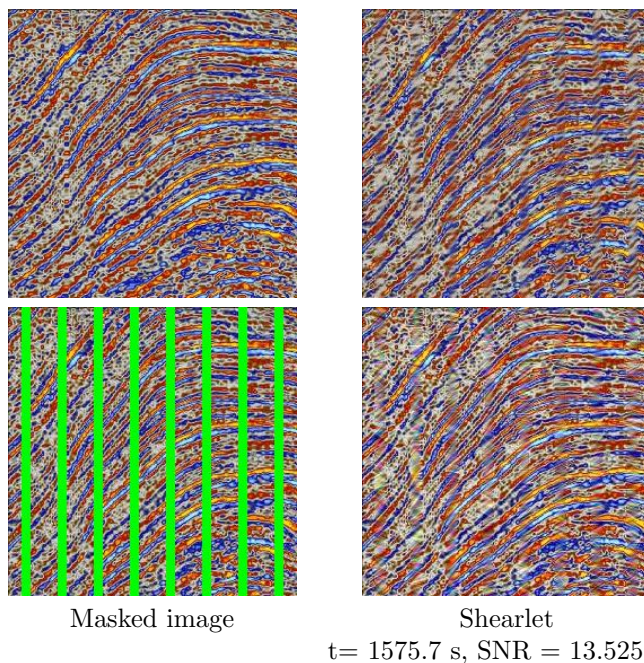


Figure 7. Top row, from left to right: seismic data, non-local means inpainting [BCM06, NLM] ( $t = 584.31$  s, SNR = 12.957 dB). Bottom row from left to right: vertical strips masked out, shearlet-based iterative thresholding ( $t = 1575.7$  s, SNR = 13.525 dB)

## ACKNOWLEDGEMENTS

Emily J. King was supported by a fellowship for postdoctoral researchers from the Alexander von Humboldt Foundation and is supported by an AMS-Simons grant. Gitta Kutyniok acknowledges support by the

Einstein Foundation Berlin, by Deutsche Forschungsgemeinschaft (DFG) Grant SPP-1324 KU 1446/13 and DFG Grant KU 1446/14, by the DFG Collaborative Research Center TRR 109 “Discretization in Geometry and Dynamics,” and by the DFG Research Center MATHEON “Mathematics for key technologies” in Berlin, Germany. Wang-Q Lim is supported by Deutsche Forschungsgemeinschaft (DFG) Grant SPP-1324 KU 1446/13 and also now DFG Collaborative Research Center TRR 109 “Discretization in Geometry and Dynamics.”

## REFERENCES

- [BBC<sup>+</sup>01] C. Ballester, M. Bertalmio, V. Caselles, G. Sapiro, and J. Verdera, *Filling-in by joint interpolation of vector fields and gray levels*, IEEE Trans. Image Process. **10** (2001), no. 8, 1200–1211.
- [BBS01] M. Bertalmio, A.L. Bertozzi, and G. Sapiro, *Navier-stokes, fluid dynamics, and image and video inpainting*, Proceedings of the 2001 IEEE Computer Society Conference on Computer Vision and Pattern Recognition, 2001 (CVPR 2001), IEEE, 2001, pp. I–355–I362.
- [BCM06] A. Buades, B. Coll, and J. M. Morel, *A review of image denoising algorithms, with a new one*, Multiscale Modeling and Simulation (SIAM interdisciplinary journal) **4** (2006), no. 2, 490–530.
- [BGN08] Lasse Borup, Rémi Gribonval, and Morten Nielsen, *Beyond coherence: recovering structured time-frequency representations*, Appl. Comput. Harmon. Anal. **24** (2008), no. 1, 120–128. MR 2379118 (2009b:94017)
- [Bha] Sooraj Bhat, *Object removal by exemplar-based inpainting*, Webpage, <http://www.cc.gatech.edu/~sooraj/inpainting/>.
- [BSCB00] M. Bertalmío, G. Sapiro, V. Caselles, and C. Ballester, *Image inpainting*, Proceedings of SIGGRAPH 2000, New Orleans, July 2000, pp. 417–424.
- [CCS10] Jian-Feng Cai, Raymond H. Cha, and Zuowei Shen, *Simultaneous cartoon and texture inpainting*, Inverse Probl. Imag. **4** (2010), no. 3, 379 – 395.
- [CDOS12] Jian-Feng Cai, Bin Dong, Stanley Osher, and Zuowei Shen, *Image restoration: Total variation, wavelet frames, and beyond*, J. Amer. Math. Soc. **25** (2012), 1033–1089.
- [Cev09] *Learning with compressible priors*, 2009 2009.
- [CPT04] A. Criminisi, P. Pérez, and K. Toyama, *Region filling and object removal by exemplar-based image inpainting*, IEEE Trans. Image Process. **13** (2004), no. 9, 1200–1212.
- [CS02] Tony F. Chan and Jianhong Shen, *Mathematical models for local nontexture inpaintings*, SIAM J. Appl. Math. **62** (2001/02), no. 3, 1019–1043 (electronic). MR 1897733 (2003f:65110)
- [DE03] David L. Donoho and Michael Elad, *Optimally sparse representation in general (nonorthogonal) dictionaries via  $l^1$  minimization*, Proc. Natl. Acad. Sci. USA **100** (2003), no. 5, 2197–2202 (electronic). MR 1963681 (2004c:94068)
- [DH01] David L. Donoho and Xiaoming Huo, *Uncertainty principles and ideal atomic decomposition*, IEEE Trans. Inform. Theory **47** (2001), no. 7, 2845–2862. MR 1872845 (2002k:94012)
- [DJL<sup>+</sup>12] Bin Dong, Hui Ji, Jia Li, Zuowei Shen, and Yuhong Xu, *Wavelet frame based blind image inpainting*, Appl. Comput. Harmon. Anal. **32** (2012), no. 2, 268–279.
- [DK13] D. L. Donoho and G. Kutyniok, *Microlocal analysis of the geometric separation problem*, Comm. Pure Appl. Math. **66** (2013), 1–47.
- [ESQD05] M. Elad, J.-L. Starck, P. Querre, and D. L. Donoho, *Simultaneous cartoon and texture image inpainting using morphological component analysis (MCA)*, Appl. Comput. Harmon. Anal. **19** (2005), no. 3, 340–358. MR 2186449 (2007h:94007)
- [Get] Webpage, [http://www.mathworks.com/matlabcentral/fileexchange/29743-tvreg-variational-image-restoration-and-segmentation/content/tvreg/tvinpaint\\_demo.m](http://www.mathworks.com/matlabcentral/fileexchange/29743-tvreg-variational-image-restoration-and-segmentation/content/tvreg/tvinpaint_demo.m).
- [GK13] P. Grohs and G. Kutyniok, *Parabolic molecules*, Found. Comput. Math. (2013), To appear.
- [GKL06] K. Guo, G. Kutyniok, and D. Labate, *Sparse multidimensional representations using anisotropic dilation und shear operators*, Wavelets und Splines (G. Chen und M. J. Lai, ed.), Nashboro Press, Nashville, TN, 2006, pp. 189–201.

- [GO] T. Goldstein and S. Osher, *The split Bregman algorithm for  $l_1$  regularized problems*, SIAM J. Imaging Sci **2**, no. 2, 323–343.
- [KKZ11] Emily J. King, Gitta Kutyniok, and Xiaosheng Zhuang, *Analysis of data separation and recovery problems using clustered sparsity*, SPIE Proceedings: Wavelets and Sparsity XIV **8138** (2011).
- [KKZ13] Emily J. King, Gitta Kutyniok, and Xiaosheng Zhuang, *Analysis of inpainting via clustered sparsity and microlocal analysis*, Journal of Mathematical Imaging and Vision (2013), To appear.
- [KL] G. Kutyniok and W. Lim, *Optimal compressive imaging for fourier data*, in preparation.
- [KL12] Gitta Kutyniok and Wang-Q Lim, *Shearlets on bounded domains*, Approximation Theory XIII: San Antonio 2010, vol. 12, Springer, 2012, pp. 187–206.
- [KT09] Matthieu Kowalski and Bruno Torr sani, *Sparsity and persistence: mixed norms provide simple signal models with dependent coefficients*, Signal, Image and Video Processing **3** (2009), 251–264.
- [Kut03] G. Kutyniok, *Geometric separation by single pass alternating thresholding*, Appl. Comput. Harmon. Anal. (2103), In press.
- [LMM11] L. Lorenzi, F. Melgani, and G. Mercier, *Inpainting strategies for reconstruction of missing data in vhr images*, IEEE Geoscience and Remote Sensing Letters **8** (2011), no. 5, 914–918.
- [NDEG11] Sangnam Nam, Michael Davies, Michael Elad, and R mi Gribonval, *Cosparsity analysis modeling - uniqueness and algorithms*, International Conference on Acoustics, Speech, and Signal Processing (ICASSP 2011), IEEE, 2011.
- [NDEG13] Sangnam Nam, Mike E. Davies, Michael Elad, and R mi Gribonval, *The Cosparsity Analysis Model and Algorithms*, Appl. Comput. Harmon. Anal. **34** (2013), no. 1, 30–56, In Press.
- [NLM] Webpage, <http://www.mathworks.com/matlabcentral/fileexchange/index?term=authorid%3A14044>.
- [Sei] Webpage, <http://www.oilandgaslawyerblog.com/2D%20seismic.JPG>.
- [SMF10] Jean-Luc Starck, Fionn Murtagh, and Jalal M. Fadili, *Sparse image and signal processing: Wavelets, curvelets, morphological diversity*, Cambridge University Press, 2010.
- [Tro04] Joel A. Tropp, *Greed is good: algorithmic results for sparse approximation*, IEEE Trans. Inform. Theory **50** (2004), no. 10, 2231–2242. MR 2097044 (2005e:94036)
- [Wei98] Joachim Weickert, *Anisotropic diffusion in image processing*, Teuber, 1998.
- [WO08] A. Wong and J. Orchard, *A nonlocal-means approach to exemplar-based inpainting*, 15th IEEE International Conference on Image Processing, 2008. ICIP 2008., IEEE, Oct 2008, pp. 2600–2603.